Reduced Mono-, Di-, and Tetracubane-Type Clusters Containing the $[MoFe_3S_4]^{2+}$ Core Stabilized by Tertiary Phosphine Ligation

Frank Osterloh, Brent M. Segal, Catalina Achim, and R. H. Holm*

Department of Chemistry and Chemical Biology, Harvard University, Cambridge, Massachusetts 02138

Received August 23, 1999

Treatment of oxidized clusters $[(Cl_4cat)(MeCN)MoFe_3S_4Cl_3]^{2-}$ (**1**) and $[(Meida)MoFe_3S_4Cl_3]^{2-}$ (**2**) with tertiary phosphines in the presence of $NaBPh_4$ in acetonitrile results in chloride substitution at the iron sites and the formation of clusters with the reduced $[MoFe_3S_4]^{2+}$ core. Thus, **1** is a precursor to $[(Cl_4cat)(MeCN)MoFe_3S_4(PR_3)_3]$ (R = Bu^t (**3**), Pr^i (**4**)) and $[(Cl_4cat)_2(Et_3P)_2Mo_2Fe_6S_8(PEt_3)_4]$ (**5**). Cluster **2** affords $[\{(Meida)MoFe_3S_4(PCy_3)_3\}_4Fe_2(\mu\text{-}Cl)L_2]^{3+}$ (L = THF (**6**), MeCN (**7**)). The structures of **3**−**7** were established by X-ray analysis. Clusters **3** and **4** are single cubanes, centrosymmetric **5** (previously reported in a different space group: Demadis, K. D.; Campana, C. F.; Coucouvanis, D. *J. Am. Chem. Soc.* **1995**, *117*, 7832) is a double cubane with a rhomboidal Fe_2S_2 bridge, and **6** and **7** are tetracubanes. In the latter, four Meida oxygen atoms from different cubanes bind each of two central high-spin Fe(II) atoms in *trans*-Fe(μ-Cl)LO_4 coordination. The topology of these clusters is not precedented. Zero-field Mössbauer parameters for all clusters are reported. Isomer shift considerations suggest the formulation $[Mo^{3+}Fe^{2+}{}_2Fe^{3+}S_4]$ for reduced clusters. Voltammetry of **3** and **4** reveals four-member electron transfer series encompassing the oxidation levels $[MoFe_3S_4]^{4+,3+,2+,+}$ in the potential interval +1.0 to −1.3 V vs SCE in dichloromethane. Compared to the clusters with monoanionic ligands at the iron sites, phosphine ligation shifts redox potentials to more positive values. This effect arises from reduction of cluster negative charge and the tendency of phosphines to stabilize lower oxidation states. The synthesis of reduced clusters **4** from **1** and of $[Fe_4S_4(PPr^i{}_3)_4]^+$ from $[Fe_4S_4Cl_4]^{2-}$ is accompanied by the formation of $Pr^i{}_3PS$, detected by ^{31}P NMR, indicating that the phosphine is the reductant. This result implies a similar function of tertiary phosphines in the synthesis of **3** and **5**−**7**. (Cl_4cat = tetrachlorocatecholate(2−); Meida = *N*-methyliminodiacetate(2−).)

Introduction

In the area of synthetic iron−sulfur[1] and molybdenum−iron−sulfur[2−4] clusters, terminal ligation by tertiary phosphines alone or in combination with other ligands has resulted in the stabilization of biologically relevant core structures with unusual oxidation levels, and of new types of core structures. Certain of these molecular aspects are not as readily obtained, or obtained at all, with conventional π-donor ligands such as thiolates, arene oxides, and halides. With $[Fe_4S_4(PR_3)_3L]$ clusters (L = halide,[5] PR_3[6]), the all-ferrous core $[Fe_4S_4]^0$ and its oxidation product $[Fe_4S_4]^+$ are stabilized relative to the usual $[Fe_4S_4]^{2+}$ state. The all-ferrous state is of particular interest because of its occurrence in the reduced iron protein of nitrogenase.[7,8] The polycubanes $[Fe_8S_8(PR_3)_6]$ and $[Fe_{16}S_{16}(PR_3)_8]$, composed of $[Fe_4S_4]^0$ units bridged by Fe−S bonds, are accessible,[6,9] but a polycubane core has not been obtained thus far with other types of terminal ligands.[10] With molybdenum−iron−sulfur clusters, the cuboidal Fe_4S_3 fragment in $[(Et_3P)MoFe_4S_6L(PEt_3)_3]$ (L = Cl^-, PhS^-)[11,12] is structurally related to the corresponding fragment in the iron−molybdenum cofactor of nitrogenase.[13,14] Similarly, the cuboidal $MoFe_3S_3$ cores in $[(Cl_4cat)MoFe_3S_3(PEt_3)_2(CO)_4]$ and $[(Cl_4cat)OMoFe_3S_3(PEt_3)_3(CO)_5]$[15] resemble the $MoFe_3S_3$ portion of the cofactor cluster. The cluster $[(Cl_4cat)_2Mo_2Fe_6S_8(PEt)_6]$[16] contains two $[MoFe_3S_4]^{2+}$ cubane-type cores linked in the manner of $[Fe_8S_8(PR_3)_6]$ to afford a rhomb-bridged double cubane. Ligand abbreviations are given in Chart 1. The entire family of structurally defined Fe−S−PR_3 clusters is summarized elsewhere.[17]

The preceding cubane-type clusters are prepared by ligand substitution reactions. Thus, the species $[Fe_4S_4(PR_3)_3L]^{+,0}$ are the products of the reaction of $[Fe_4S_4L_4]^{2-}$ (L = halide) with R_3P,[5,6] and $[(Cl_4cat)_2Mo_2Fe_6S_8(PEt)_6]$ is obtained from $[(Cl_4cat)(MeCN)MoFe_3S_4Cl_3]^{2-}$ and Et_3P.[16] These reactions afford

(1) Beinert, H.; Holm, R. H.; Münck, E. *Science* **1997**, *277*, 653.
(2) Holm, R. H.; Simhon, E. D. In *Molybdenum Enzymes*; Spiro, T. G., Ed.; Wiley-Interscience: New York, 1985; Chapter 1.
(3) Coucouvanis, D. *Acc. Chem. Res.* **1991**, *24*, 1.
(4) Holm, R. H. *Adv. Inorg. Chem.* **1992**, *38*, 1.
(5) Tyson, M. A.; Demadis, K. D.; Coucouvanis, D. *Inorg. Chem.* **1995**, *34*, 4519.
(6) Goh, C.; Segal, B. M.; Huang, J.; Long, J. R.; Holm, R. H. *J. Am. Chem. Soc.* **1996**, *118*, 11844.
(7) Watt, G. D.; Reddy, K. R. N. *J. Inorg. Biochem.* **1994**, *53*, 281.
(8) Yoo, S. J.; Angove, H. C.; Burgess, B. K.; Hendrich, M. P.; Münck, E. *J. Am. Chem. Soc.* **1999**, *121*, 2534 and references therein.
(9) Cai, L.; Segal, B. M.; Long, J. R.; Scott, M. J.; Holm, R. H. *J. Am. Chem. Soc.* **1995**, *117*, 8863.
(10) Note, however, that a somewhat similar Fe_8S_8 core has been stabilized by another type of π-acid ligand in $[Fe_8S_8(ArNC)_{18}]^{2+}$: Harmjanz, M.; Saak, W.; Haase, D.; Pohl, S. *Chem. Commun. (Cambridge)* **1997**, 951.
(11) Nordlander, E.; Lee, S. C.; Cen, W.; Wu, Z. Y.; Natoli, C. R.; Di Cicco, A.; Filipponi, A.; Hedman, B.; Hodgson, K. O.; Holm, R. H. *J. Am. Chem. Soc.* **1993**, *115*, 5549.
(12) Cen, W.; MacDonnell, F. M.; Scott, M. J.; Holm, R. H. *Inorg. Chem.* **1994**, *33*, 5809.
(13) Howard, J. B.; Rees, D. C. *Chem. Rev.* **1996**, *96*, 2965.
(14) Peters, J. W.; Stowell, M. H. B.; Soltis, S. M.; Finnegan, M. G.; Johnson, M. K.; Rees, D. C. *Biochemistry* **1997**, *36*, 181.
(15) Tyson, M. A.; Coucouvanis, D. *Inorg. Chem.* **1997**, *36*, 3808.
(16) Demadis, K. D.; Campana, C. F.; Coucouvanis, D. *J. Am. Chem. Soc.* **1995**, *117*, 7832.
(17) Goddard, C. A.; Long, J. R.; Holm, R. H. *Inorg. Chem.* **1996**, *35*, 4347.

10.1021/ic991016x CCC: $19.00
Published on Web 02/12/2000

Chart 1. Designation of Compounds[a]

$[(Cl_4cat)(MeCN)MoFe_3S_4Cl_3]^{2-}$	**1**[22]
$[(Meida)MoFe_3S_4Cl_3]^{2-}$	**2**[23,24]
$[(Cl_4cat)(MeCN)MoFe_3S_4(PBu^t_3)_3]$	**3**
$[(Cl_4cat)(MeCN)MoFe_3S_4(PPr^i_3)_3]$	**4**
$[(Cl_4cat)_2(Et_3P)_2Mo_2Fe_6S_8(PEt_3)_4]$	**5**[16]
$[\{Meida)MoFe_3S_4(PCy_3)_3\}_4Fe_2(\mu\text{-}Cl)(THF)_2]^{3+}$	**6**
$[\{Meida)MoFe_3S_4(PCy_3)_3\}_4Fe_2(\mu\text{-}Cl)(MeCN)_2]^{3+}$	**7**
$[(al_2cat)(EtCN)MoFe_3S_4(S\text{-}p\text{-}C_6H_4Cl)_3]^{3-}$	**8**[19]
$[(al_2cat)(p\text{-}ClC_6H_4S)MoFe_3S_4(S\text{-}p\text{-}C_6H_4Cl)_3]^{3-}$	**9**[40]
$[(al_2cat)(THF)MoFe_3S_4Cl_3]^{2-}$	**10**[22]
$[(al_2cat)(MeCN)MoFe_3S_4(S\text{-}p\text{-}C_6H_4Cl)_3]^{2-}$	**11**[40]

Abbreviations: al_2cat 3,6-diallylcatecholate(2-); Cl_4cat tetrachlorocatecholate(2-); Cy cyclohexyl; Meida N-methyliminodiacetate(2-); pta 1,3,5-triaza-7-phosphaadamantane

[a] Ligands bound to molybdenum precede Mo.

products with the *reduced* cores $[Fe_4S_4]^+$ and $[MoFe_3S_4]^{2+}$. While clusters in these oxidation levels are accessible by chemical reduction of $[Fe_4S_4]^{2+}$ [18] and $[MoFe_3S_4]^{3+}$ [19] precursors and by direct synthesis ($[Fe_4S_4]^+$),[20] their oxidative instability is indicated by redox potentials of $\lesssim -1.0$ V vs SCE. In the synthetic reactions, the probable reductant is the tertiary phosphine. Indeed, R_3PS has been detected (but not quantitated) among reaction products by IR spectroscopy[5] and mass spectrometry.[6] Recently, we have proposed that, because the cofactor ($Fe^{2.14+}$) and P-cluster (Fe^{2+}) of nitrogenase are substantially or completely reduced with the indicated (mean) oxidation states likely, profitable synthetic approaches to them might utilize stable reduced clusters as precursors.[21] As one example, reaction of $[(Cl_4cat)_2Mo_2Fe_6S_8(PEt)_6]$ and hydrosulfide yields the high-nuclearity cluster $[(Cl_4cat)_6(Et_3P)_6Mo_6Fe_{20}S_{30}]^{8-}$, which contains fragments whose topology provides the closest approach to that of the P-cluster.[21] Because of this and related synthetic results in this laboratory, we have examined the formation, structures, and certain electronic features of reduced clusters stabilized by terminal phosphine ligation. The principal findings of that investigation are reported here.

Experimental Section

Preparation of Compounds. All operations were carried out under a pure dinitrogen atmosphere using standard inert atmosphere box or Schlenk techniques. Solvents were dried and degassed before use. Unless referenced, compounds were of commercial origin and were used as received.

$[(Cl_4cat)(MeCN)MoFe_3S_4(PBu^t_3)_3]$. To a stirred solution of 1.00 g (0.956 mmol) of $(Et_4N)_2[(Cl_4cat)(MeCN)MoFe_3S_4Cl_3]$[22,23] in 12 mL of acetonitrile was added a solution of 0.773 g (3.82 mmol) of PBu^t_3 in 1 mL of benzene, followed by a solution of 0.981 g (2.87 mmol) of $NaBPh_4$ in 5 mL of acetonitrile. The resulting dark brown solution was allowed to stand for 2 days at room temperature. Black crystals formed together with a white precipitate (NaCl). The mother liquor was decanted off, and acetonitrile was added to the remaining solids. The mixture was agitated, and the solvent with suspended NaCl was decanted. The process was repeated twice (2 × 15 mL). The crude product was collected, dried in vacuo, and recrystallized from dichloromethane/acetonitrile to afford the product as 0.730 g (56%) of black crystals of the $\cdot 3CH_2Cl_2$ solvate. An analytical sample of the unsolvated compound was obtained by drying the solvated material overnight in vacuo. IR (KBr): 1433 cm^{-1} (s, Cl_4cat). ^1H NMR ($CDCl_3$): δ 1.40 (Me), 6.70 (Bu^t). FAB-MS^+: *m*/*z* 1243 ($[M - MeCN]^+$). Anal. Calcd for $C_{47}H_{90}Cl_{10}Fe_3MoNO_2P_3S_4$: C, 41.11; H, 6.59; Fe, 13.03; Mo, 7.46; P, 7.23; S, 9.98. Found: C, 40.73; H, 6.78; Fe, 13.26; Mo, 7.54; P, 7.31; S, 10.25.

$[(Cl_4cat)(MeCN)MoFe_3S_4(PPr^i_3)_3]$. The preceding method was employed with 0.350 g (0.335 mmol) of $(Et_4N)_2[(Cl_4cat)(MeCN)MoFe_3S_4Cl_3]$, 0.245 g (1.53 mmol) of PPr^i_3, and 0.345 g (1.00 mmol) of $NaBPh_4$ in a total of 9 mL of acetonitrile. Recrystallization from dichloromethane/acetonitrile gave the product as 0.191 g (49%) of black crystals. IR (KBr): 1439 cm^{-1} (s, Cl_4cat). ^1H NMR ($CDCl_3$): δ 1.44 (MeCN), 5.51 ($CHMe_2$), 14.43 ($CHMe_2$). FAB-MS^+: *m*/*z* 1118 ($[M - MeCN]^+$). Anal. Calcd for $C_{35}H_{66}Cl_4Fe_3MoNO_2P_3S_4$: C, 36.26; H, 5.74; Fe, 14.45; Mo, 8.28; N, 1.21; P, 8.01; S, 11.06. Found: C, 36.38; H, 5.64; Fe, 14.79; Mo, 8.68; N, 1.26; P, 8.22; S, 11.22.

$[(Cl_4cat)_2Mo_2Fe_6S_8(PEt_3)_6]$. The preparation of this compound has been briefly described;[16] a more detailed procedure is given here. To a stirred solution of 4.00 g (3.84 mmol) of $(Et_4N)_2[(Cl_4cat)(MeCN)MoFe_3S_4Cl_3]$ in 800 mL of acetonitrile was added 1.80 g (15.2 mmol) of PEt_3 followed by a solution of 3.88 g (11.3 mmol) of $NaBPh_4$ in 20 mL of acetonitrile. The reaction mixture was allowed to stand for 3 days, during which time black crystals and NaCl separated. The mother liquor was decanted, and 30 mL of acetonitrile was added to the solid. The mixture was agitated, and solvent with suspended NaCl was decanted. The process was repeated twice (2 × 30 mL). The black solid was collected, washed with dichloromethane (2 × 10 mL), and dried in vacuo to give 2.00 g (59%) of product as a pyrophoric black crystalline solid. An analytical sample was recrystallized from dichloromethane/acetonitrile. IR (KBr): 1446 cm^{-1} (s, Cl_4cat). ^1H NMR ($CDCl_3$): δ 2.05 ($FePCH_2Me$), 2.19 ($MoPCH_2Me$), 6.94 ($MoPCH_2$); 7.77, 10.21 ($FePCH_2$). Anal. Calcd for $C_{48}H_{90}Cl_8Fe_6Mo_2O_4P_6S_8$: C, 29.06; H, 4.57; Fe, 16.89; Mo, 9.67; P, 9.37; S, 12.93. Found: C, 28.71; H, 4.61; Fe, 17.37; Mo, 9.86; P, 9.63; S, 13.42.

$[\{(Meida)MoFe_3S_4(PCy_3)_3\}_4Fe_2(\mu\text{-}Cl)(THF)_2](BPh_4)_3$. To a stirred solution of 1.05 g (1.01 mmol) of $(Et_4N)_2[(Meida)MoFe_3S_4Cl_3]$[23,24] in 60 mL of acetonitrile was added a solution of 1.47 g (5.05 mmol) of PCy_3 in 15 mL of THF, followed by a solution of 1.20 g (4.26 mmol) of $NaBPh_4$ in 15 mL of acetonitrile. A black crystalline solid began to form after 10 min. After 30 h, the supernatant liquid was decanted, and 10 mL of acetonitrile was added to the solid. The mixture was agitated, and the suspension of NaCl in acetonitrile was decanted. The step was repeated twice (2 × 10 mL). The black solid was dried in vacuo to give 1.08 g of crude product, which is a mixture of the title compound and $[\{(Meida)MoFe_3S_4(PCy_3)_3\}_4Fe_2(\mu\text{-}Cl)(MeCN)_2](BPh_4)_3$ (vide infra). The crude product was extracted with 2.5 mL of THF, the extract was filtered, and an equal volume of cyclohexane was added. Storage at room temperature for 24 h afforded black rhombs, which were collected, washed with THF, and dried in vacuo to afford the product as 0.40 g (23%) of black crystalline solid. IR (KBr): ν_{COO} 1611 cm^{-1}. FAB-MS^+: *m*/*z* 1379 ($[(Meida)MoFe_3S_4(PCy_3)_3]^+$). This compound was identified by an X-ray structure determination.

$[\{(Meida)MoFe_3S_4(PCy_3)_3\}_4Fe_2(\mu\text{-}Cl)(MeCN)_2](BPh_4)_3$. The crude product from the preceding preparation, after being extracted with THF, was dried in vacuo. This material was dissolved in the minimal volume

(18) Carney, M. J.; Papefthymiou, G. C.; Whitener, M. A.; Spartalian, K.; Frankel, R. B.; Holm, R. H. *Inorg. Chem.* **1988**, *27*, 346.
(19) Mizobe, Y.; Mascharak, P. K.; Palermo, R. P.; Holm, R. H. *Inorg. Chim. Acta* **1983**, *80*, L65.
(20) Hagen, K. S.; Watson, A. D.; Holm, R. H. *Inorg. Chem.* **1984**, *23*, 2984.
(21) Osterloh, F.; Sanakis, Y.; Staples, R. J.; Münck, E.; Holm, R. H. *Angew. Chem., Int. Ed.* **1999**, *38*, 2066.
(22) Palermo, R. E.; Holm, R. H. *J. Am. Chem. Soc.* **1983**, *105*, 4310.
(23) Huang, J.; Mukerjee, S.; Segal, B. M.; Akashi, H.; Zhou, J.; Holm, R. H. *J. Am. Chem. Soc.* **1997**, *119*, 8662.
(24) Demadis, K. D.; Coucouvanis, D. *Inorg. Chem.* **1995**, *34*, 436.

Table 1. Crystallographic Data for Clusters[a]

	3·3CH_2Cl_2	**4**	**5**[d]	[**7**]$(BPh_4)_3$·2CH_3CN
formula	$C_{47}H_{90}Cl_{10}Fe_3MoNO_2P_3S_4$	$C_{35}H_{66}Cl_4Fe_3MoNO_2P_3S_4$	$C_{48}H_{90}C_{l8}F_5Mo_2O_4P_6S_8$	$C_{316}H_{496}B_3ClFe_{14}Mo_4N_8O_{16}P_{12}S_{16}$
fw, g·mol^{-1}	1540.34	1159.33	1984.08	6781.58
cryst syst	monoclinic	orthorhombic	triclinic	tetragonal
space group	$P2/c$	$Pna2_1$	$P\bar{1}$	$P4/ncc$
Z	4	4	2	4
a, Å	13.545(3)	23.493(1)	13.549(3)	32.9623(3)
b, Å	22.339(5)	11.4994(6)	14.114(3)	
c, Å	23.070(5)	18.265(1)	23.654(5)	35.6578(4)
α, deg			76.04(3)	
β, deg	106.45(3)		86.02(3)	
γ, deg			62.57(3)	
V, Å	6695(2)	4934.2(4)	3892(1)	38743(1)
d_{calc}, g·cm^{-3}	1.528	1.561	1.693	1.217
μ, mm^{-1}	1.451	1.627	2.046	0.823
T, K	213	213	213	213
θ range, deg	1.81−25.00	1.97−27.76	0.89−26.56	1.44−22.50
GOF (F^2)	1.033	1.024	1.086	1.075
R1,[b] wR2[c]	0.0319, 0.0806	0.0714, 0.1348	0.0579, 0.1465	0.0684, 0.2129

[a] Collected using Mo Kα ($\lambda = 0.71073$ Å) radiation. [b] $R1 = \sum||F_o| - |F_c||/\sum|F_o|$. [c] $wR2 = \{\sum[w(F_o^2 - F_c^2)^2]/\sum[w(F_o^2)^2]\}^{1/2}$. [d] Also reported in monoclinic space group $P2_1/c$, $a = 25.554(4)$ Å, $b = 12.740(2)$ Å, $c = 26.634(5)$ Å, $\beta = 112.405(4)°$, $V = 8016(2)$ Å^3, $Z = 4$ and in triclinic space group $P\bar{1}$ with $a = 12.1377(6)$ Å, $b = 13.6889(6)$ Å, $c = 13.7462(2)$ Å, $\alpha = 64.053(3)°$, $\beta = 78.972(3)°$, $\gamma = 86.153(3)°$, $V = 2016.45(6)$ Å^3, $Z = 2$.[16] Based on volume considerations, it is probable that $Z = 1$ for the triclinic form.

of dichloromethane (ca. 1 mL), and 3 mL of acetonitrile was added to the extract. The black solution was maintained at room temperature for 1 day, during which time black tetragonal crystals formed. The crystalline solid was collected, washed with acetonitrile, and dried in vacuo to give 0.60 g (39%) of product. IR (KBr): ν_{COO} 1674 (sh), 1604 cm^{-1}. FAB-MS$^+$: m/z 1379 ([(Meida)$MoFe_3S_4(PCy_3)_3$]$^+$). ^{1}H NMR (CD_2Cl_2, cation): δ −1.0 (NMe), 0.6−4.3 (m, Cy), 5.78 (PCH); 15.5, 20.4 (CH_2). Anal. Calcd for $C_{312}H_{490}B_3ClFe_{14}Mo_4N_8O_{16}P_{12}S_{16}$: C, 55.93; H, 7.37; Cl, 0.53; Fe, 11.67; Mo, 5.73; P, 5.55; S, 7.66. Found: C, 54.47; H, 7.31; Fe, 11.48; Mo, 5.70; P, 5.65; S, 7.59.

X-ray Structure Determinations. Crystal structures were determined for the four compounds in Table 1. Hereafter, clusters are designated as in Chart 1. Crystals of **3**·3CH_2Cl_2, **5**, and [**7**]$(BPh_4)_3$·2MeCN were obtained by recrystallization from dichloromethane/acetonitrile. A suitable crystal of **4** was obtained directly from the reaction mixture. Crystals were coated with Paratone oil and glued to glass fibers with Apiezon L grease, and were transferred to a Siemens SMART diffractometer and cooled in a nitrogen stream (−60 °C). Data were measured using ω scans of 0.3° per frame, such that a hemisphere was collected. A total of 1271 frames were collected with a maximum resolution of 0.75 Å. The first 50 frames were re-collected at the end of the data collection to monitor for decay; none was found. Cell parameters were retrieved using SMART software and refined using SAINT on all observed reflections. Data reduction was performed with SAINT software which corrects for Lorentz polarization and decay. Absorption corrections were applied using SADABS. Structures were solved by direct methods using SHELXS-97 and refined by least squares on F^2 (SHELXL-97). Unless stated otherwise, non-hydrogen atoms were described anisotropically. Hydrogen atoms were placed in idealized positions and refined employing a riding model with thermal parameters 1.2× those of the bond carbon atoms.

The structure of **4** was originally solved in centrosymmetric space group *Pnma* but could not be fully refined owing to disorder of the isopropyl groups of one ligand. Refinement in orthorhombic space group $Pna2_1$ using a racemic twin model and employing the TWIN statement in SHELXL-97 proceeded satisfactorily and resulted in a BASF (relative batch scale factor) of 0.449. In this model, all non-hydrogen atoms except carbon atoms were refined anisotropically, and the carbon atoms of one phosphine ligand were refined with fixed C−C bond distances. Compound **5** contains two molecules in the unit cell, each being located on a crystallographic inversion center. The cluster cation of [**7**]$(BPh_4)_3$·2MeCN is located on a crystallographic 4-fold axis. Acetonitrile ligands to the central iron atoms were disordered along the 4-fold axis and were refined without hydrogen atoms. Acetonitrile solvate molecules were refined with half-occupancy. Initially, the anion in the asymmetric unit was refined with full occupancy, corresponding to 4 anions/cation. After it was found that a 4+ cation is not consistent with the ^{57}Fe Mössbauer spectra (vide infra), the anion occupancy was refined as a free variable. The model converged at an occupancy of 0.74, indicating a 3+ cation and 3 anions and gave improved agreement factors (Table 1) compared to the model with unit anion occupancy (R1 = 0.0728, wR2 = 0.2109, GOF = 1.129). Crystallographic data are collected in Table 1. (See paragraph at the end of this paper concerning Supporting Information available.)

The compound [**6**]$(BPh_4)_3$, crystallized from THF/cyclohexane and obtained as the ·7THF·3C_6H_{12} solvate, occurred in triclinic space group $P\bar{1}$ with $a = 23.3240(3)$ Å, $b = 26.2333(1)$ Å, $c = 34.3355(5)$ Å, $\alpha = 91.363°$, $\beta = 105.705°$, $\gamma = 102.822°$, $V = 19641$ Å^3, $Z = 2$. The structure contains 450 independent atoms. It was refined to the point where atom connectivity was fully established and metric parameters were found to be very similar to those of **7**. The only significant structural difference with **7** is the presence of two axial THF molecules at the central iron atoms.

Other Physical Measurements. All measurements were made under anaerobic conditions. IR spectra were determined with a Nicolet Impact 400 FT-IR instrument. ^{1}H and ^{31}P NMR spectra were obtained with Bruker AM-400/500 spectrometers. ^{31}P shifts are relative to external 85% D_3PO_4. Mass spectra were recorded on a JEOL SX-102 spectrometer; for FAB spectra, 3-nitrobenzyl alcohol was used as the matrix. Electrochemical measurements were performed with a PAR model 263 potentiostat/galvanostat using a Pt working electrode and 0.1 M (Bu_4N)(PF_6) supporting electrolyte in dichloromethane solution. Potentials are reported vs SCE. Mössbauer spectra were recorded on a constant-acceleration spectrometer. Isomer shifts are reported with respect to iron metal at room temperature. Data were analyzed using WMOSS software (WEB Research Co., Edina, MN).

Results and Discussion

Synthesis and Structures of Clusters. In seeking reduced clusters stabilized by phosphine ligation, the reactions in Figure 1 based on conventional, thoroughly characterized $[MoFe_3S_4]^{3+}$ ($S = {}^3/_2$) clusters **1** and **2**[22−24] were examined. Depending on the phosphine, reactions of **1** in acetonitrile yield single or double cubanes. Phosphines with large cone angles (PBu^t_3, 182°; PPr^i_3, 160°)[25] afford the single cubanes **3** (56%) and **4** (49%) in the indicated yields. Use of Et_3P (132°)[25] in a closely related

(25) pK_a values and cone angles of phosphines: PEt_3, 8.69, 132°; PPr^i_3, —, 160°; PCy_3, 9.70, 170°; PBu^t_3, 11.4, 182°. Cf.: Rahman, M. M.; Liu, H. Y.; Prock, A.; Giering, W. P. *Organometallics* **1987**, *6*, 650 and references therein.

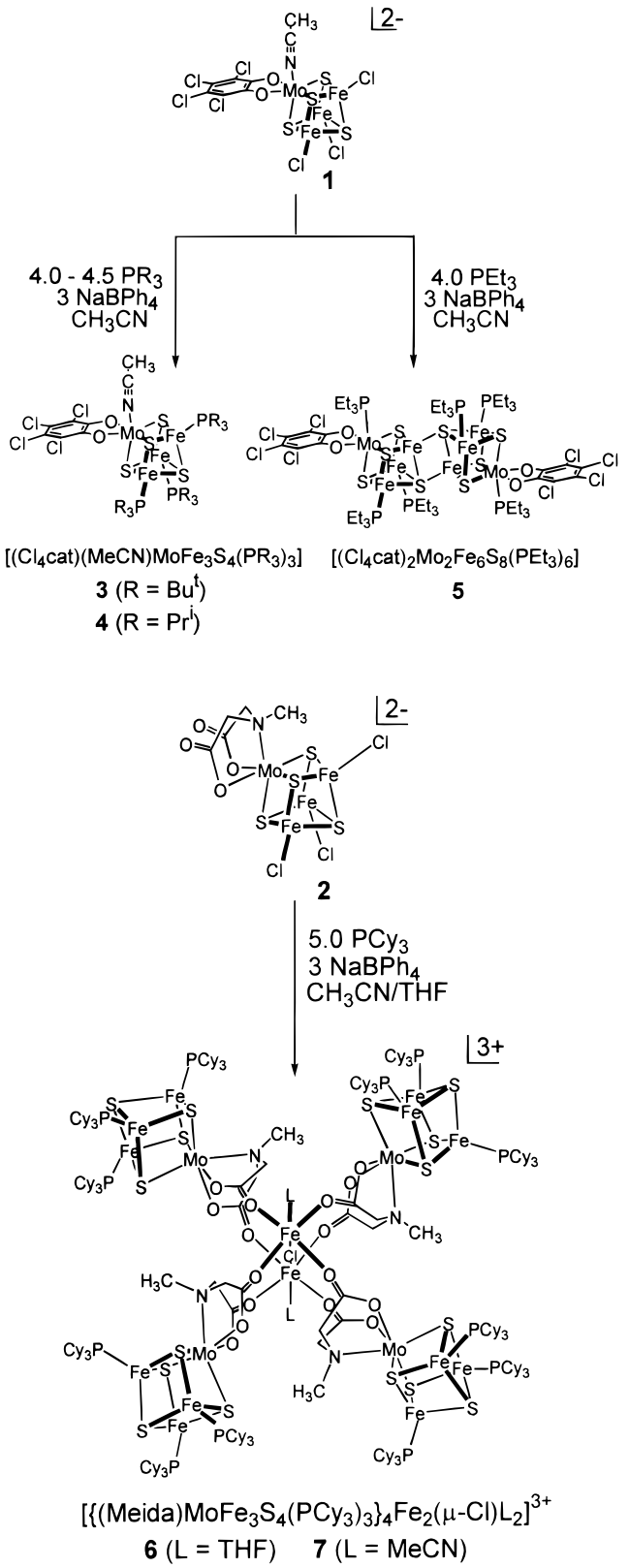

Figure 1. Schematic representation of the synthesis of phosphine-substituted clusters: single cubanes **3** and **4** and fused double cubane **5** from cluster **1**, and tetracubanes **6** and **7** from cluster **2.**

reaction scheme results in the double cubane **5** (59%), as first reported by Demadis et al.[16] The three clusters contain reduced core units ($[MoFe_3S_4]^{2+}$), in agreement with their composition and as demonstrated by Mössbauer spectroscopy (vide infra). Reactions 1 and 2 provide the simplest stoichiometry consistent with the observed cluster products. The reactions are conducted

$$2[(Cl_4cat)(MeCN)MoFe_3S_4Cl_3]^{2-} + 4R_3P + 6NaBPh_4 \rightarrow [(Cl_4cat)(MeCN)MoFe_3S_4(PR_3)_3] + R_3PS + 6NaCl + 6BPh_4^- + \text{“}[(Cl_4cat)MoFe_3S_3]^{2+}\text{”} \quad (1)$$

$$3[(Cl_4cat)(MeCN)MoFe_3S_4Cl_3]^{2-} + 7Et_3P + 9NaBPh_4 \rightarrow [(Cl_4cat)_2(Et_3P)_2Mo_2Fe_6S_8(PEt_3)_4] + Et_3PS + 9NaCl + 9BPh_4^- + \text{“}[(Cl_4cat)MoFe_3S_3]^{3+}\text{”} \quad (2)$$

in acetonitrile. In practice, $NaBPh_4$ (soluble in acetonitrile) is added to the reaction systems to assist removal of bound chloride as insoluble NaCl. The products in quotes serve to balance the reactions and are otherwise fictitious. In both reactions, the core of one starting cluster is compromised by removal of 1 equiv of sulfide to form R_3PS and to generate two electrons. According to reaction 1, it is assumed that one electron is captured by **1** with accompanying substitution of chloride by phosphine at the tetrahedral iron sites, yielding the product **3** or **4.** The other electron is taken up by an unidentified metal-containing fragment of the compromised cluster. In reaction 2, two clusters **1** are reduced with concomitant phosphine binding at molybdenum and iron sites and development of Fe−S bridge bonds to form the double cubane **5**. Based on reactions **1** and **2**, excess phosphine was used in the preparations of **3** and **4.** However, the acetonitrile ligand of **1** is retained when the large cone angles of the phosphines[25] preclude binding at an octahedral molybdenum site. The smaller cone angle of Et_3P allows binding at two such sites in **5**.

Reaction of cluster **2** with different phosphines was examined, but Cy_3P gave the most tractable product. Surprisingly, the product is not a single cubane but instead an unprecedented tetracubane cluster. The reaction mixture specified in Figure 1 afforded a black crystalline solid which precipitated over the course of 24 h. Extraction of this material with THF and crystallization of the extracted product from THF/cyclohexane affords the compound $[\mathbf{6}](BPh_4)_3$ as a THF/cyclohexane solvate (23%) in the form of black triclinic rhombs. Crystallization of the extraction residue from acetonitrile/dichloromethane gave $[\mathbf{7}](BPh_4)_3 \cdot 2MeCN$ as black tetragonal blocks (39%). In both compounds, the central iron atoms are Fe(II) from Mössbauer spectroscopy which, with a bridging chloride ligand, requires that all cubane units are in the $[MoFe_3S_4]^{2+}$ oxidation state. Formation of these clusters requires sacrifice of at least $^1/_2$ equiv of starting cluster to afford 2Fe(II), chloride, and the four electrons from two sulfides needed to constitute **6** or **7**. Because of the complexity of the process, no reaction stoichiometry is offered.

Cluster Structures. Crystal structures have been determined for clusters **3**−**7**. Selected metric data are summarized in Tables 2 and 3. The structure of **3** is presented in Figure 2; that of **4** is similar and is not shown. The cluster is a single cubane with idealized mirror symmetry. The iron sites exhibit distorted tetrahedral $FePS_3$ coordination with P−Fe−S = 107.1−116.8° and mean Fe−P = 2.45(4) Å. The latter value is indistinguishable from those found for $[Fe_4S_4(PBu^t_3)_3Cl]$[5] and $[Fe_4S_4(PBu^t_3)_4]^+$.[6] The molybdenum atom is bound in a distorted octahedral $MoNO_2S_3$ arrangement with mean bond lengths Mo−O = 2.104(1) Å and Mo−S = 2.360(3) Å, and nearly linear acetonitrile coordination with Mo−N = 2.277(3) Å and Mo−N−C = 172.1(3)°. The Mo−O and Mo−S bond distances are very similar to those of oxidized clusters **2**[24] and **10**.[22] For example, in **10** Mo−O = 2.045(4) Å and Mo−S = 2.36(2) Å.

Previously, the structure of double cubane **5** in monoclinic space group $P2_1/c$ was summarized and cell parameters of a triclinic ($P\bar{1}$) modification were reported.[16] We also have

Table 2. Selected Interatomic Distances (Å) and Angles (deg) for [(Cl_4cat)(MeCN)$MoFe_3S_4$(PBu^t_3)$_3$] (**3**·$3CH_2Cl_2$), [(Cl_4cat)(MeCN)$MoFe_3S_4$(PPr^i_3)$_3$] (**4**), [(Cl_4cat)$_2$(Et_3P)$_2Mo_2Fe_6S_8$(PEt_3)$_4$] (**5**), and [{(Meida)$MoFe_3S_4$(PCy_3)$_3$}$_4Fe_2$(μ-Cl)(MeCN)$_2$](BPh_4)$_3$ ([**7**](BPh_4)$_3$·$2CH_3CN$)

	3·$3CH_2Cl_2$	**4**	**5**[a]		[**7**](BPh_4)$_3$·$2CH_3CN$	
Mo(1)−Fe(1)	2.7275(7)	2.681(1)		2.68(1)		2.684(1)
Mo(1)−Fe(2)	2.7050(8)	2.696(4)		2.674(2)		2.667(1)
Mo(1)−Fe(3)	2.7121(8)	2.667(4)		2.657(4)		2.661(1)
Fe(1)−Fe(2)	2.692(1)	2.632(5)		2.641(8)		2.633(2)
Fe(1)−Fe(3)	2.6962(8)	2.596(5)		2.621(4)		2.618(2)
Fe(2)−Fe(3)	2.6900(8)	2.628(2)		2.610(8)		2.668(2)
N(1)−C(43)	1.134(4)	1.14(1)	Fe(1)−Fe(1′)[b]	2.639(2)		
Mo(1)−O(1)	2.105(2)	2.05(2)		2.090(3)	Mo(1)−O(1)	2.132(5)
Mo(1)−O(2)	2.103(2)	2.14(2)		2.095(8)	Mo(1)−O(3)	2.129(5)
Mo(1)−N(1)	2.277(3)	2.280(9)	Mo(1)−P(1)	2.597(2)		2.299(6)
Mo(1)−S(1)	2.3617(9)	2.356(2)		2.430(6)		2.360(2)
Mo(1)−S(2)	2.361(1)	2.344(7)		2.362(6)		2.342(2)
Mo(1)−S(3)	2.3560(9)	2.398(8)		2.376(5)		2.364(2)
Fe(1)−S(2)	2.267(1)	2.236(8)		2.253(4)		2.262(2)
Fe(1)−S(3)	2.270(1)	2.278(9)		2.253(6)		2.251(2)
Fe(1)−S(4)	2.307(1)	2.282(3)		2.367(3)		2.288(2)
Fe(1)−P(1)	2.497(1)	2.380(2)	Fe(1)−S(4′)	2.245(4)		2.415(2)
Fe(2)−S(1)	2.252(1)	2.254(7)		2.241(4)		2.231(2)
Fe(2)−S(3)	2.2578(9)	2.269(8)		2.227(1)		2.246(2)
Fe(2)−S(4)	2.290(1)	2.267(7)		2.316(1)		2.232(2)
Fe(2)−P(2)	2.445(1)	2.344(9)		2.350(1)		2.344(3)
Fe(3)−S(1)	2.253(1)	2.229(6)		2.234(6)		2.237(2)
Fe(3)−S(2)	2.255(1)	2.218(7)		2.229(2)		2.268(2)
Fe(3)−S(4)	2.2667(9)	2.257(8)		2.322(2)		2.288(2)
Fe(3)−P(3)	2.418(1)	2.368(8)		2.351(3)		2.394(2)
O(1)−Mo(1)−O(2)	77.35(8)	77.6(3)		76.76(7)	O(1)−Mo(1)−O(3)	78.3(2)
O(1)−Mo(1)−N(1)	81.74(9)	81.1(7)	O(1)−Mo(1)−P(1)	84(2)	O(1)−Mo(1)−N(1)	76.1(2)
O(2)−Mo(1)−N(1)	77.94(9)	78.9(6)	O(2)−Mo(1)−P(1)	83(1)	O(3)−Mo(1)−N(1)	76.0(2)
N(1)−Mo(1)−S(1)	167.10(7)	166.2(2)	S(1)−Mo(1)−P(1)	168(1)	N(1)−Mo(1)−S(1)	158.9(2)
S(2)−Fe(1)−P(1)	113.58(4)	112.7(3)	S(4′)−Fe(1)−S(2)	110.9(4)	S(2)−Fe(1)−P(1)	110.78(8)
S(3)−Fe(1)−P(1)	110.59(3)	111.5(3)	S(4′)−Fe(1)−S(3)	114(1)	S(3)−Fe(1)−P(1)	114.19(9)
S(4)−Fe(1)−P(1)	115.52(4)	111.0(1)	S(4′)−Fe(1)−S(4)	110.3(7)	S(4)−Fe(1)−P(1)	111.08(9)
S(1)−Fe(2)−P(2)	114.15(3)	112.1(3)		108(1)		104.10(9)
S(3)−Fe(2)−P(2)	107.13(4)	112.1(3)		113(2)		110.73(9)
S(4)−Fe(2)−P(2)	116.80(4)	111.5(3)		111(1)		120.62(9)
S(1)−Fe(3)−P(3)	113.24(3)	109.2(3)		116.0(9)		111.03(9)
S(2)−Fe(3)−P(3)	109.47(4)	110.4(3)		108.9(1)		104.59(8)
S(4)−Fe(3)−P(3)	114.99(4)	114.6(3)		106(1)		121.59(9)
Mo(1)−N≡C	172.1(3)	178(2)	Fe(1′)−S(4)−Fe(1)	69.7(7)		

[a] Mean values for two independent molecules. [b] Symmetry transformations used to generate equivalent atoms for the two independent molecules in the unit cell: $-x, -y+1, -z+1$ and $-x+2, -y+3, -z$.

obtained the compound in the latter space group but with different cell dimensions. The cluster structure in our triclinic modification is shown in Figure 3. The cluster is centrosymmetric, requiring a trans disposition of the two molybdenum sites (Mo(1)···Mo(1′) = 7.86(4) Å). The two cubanes are linked by an Fe(1,1′)S(4,4′) planar rhomb with Fe(1)−S(4) = 2.367(3) Å, Fe(1)−S(4′) = 2.245(4) Å, and Fe(1)−Fe(1′) = 2.639(2) Å. The prevalent bond distance order Fe(1)−(μ_4-S) > Fe−(μ_3-S) is followed except for Fe(1)−S(4′), which is comparable to the six intracubane Fe−S distances (mean 2.24(1) Å). This property suggests a bridge bond strength commensurate with intracubane Fe−S bonds. The bridging mode is precedented in [Fe_8S_8(PCy_3)$_6$], in which the bridge rhomb distances and angles are similar to those of **5**.[6,9] Overall, molecular parameters of the monoclinic and triclinic forms of **5** are not significantly different. While examples are not numerous, the Fe_2S_2 rhombic bridge has been observed only in *reduced* clusters ([Fe_4S_4]^0, [$MoFe_3S_4$]$^{2+}$) where the nucleophilicity of a core sulfide atom is sufficient to sustain four bridging interactions.

The structures of tetracubanes **6** and **7**, shown in Figure 4, could only have been established by X-ray determinations. The two clusters differ compositionally in the axial ligand attached to the central iron atoms and structurally are essentially identical. For this reason, only the fully refined structure of **7** is reported. The cluster is a trication containing four [$MoFe_3S_4$]$^{2+}$ cubanes whose iron sites have distorted tetrahedral $FePS_3$ stereochemistry. The molybdenum sites contain Meida coordinated as a facial tridentate ligand in a distorted octahedral $MoNO_2S_3$ fragment. Dimensions of individual cubanes are similar to those of **3** and **4**. The central portion of the cluster is depicted in Table 3 together with bond distances and angles. Each central Fe(II) site has tetragonally distorted octahedral $FeClNO_4$ coordination. The four oxygen atoms derive from the Meida ligands of four different cubanes, and the nitrogen atom derives from a linearly coordinated acetonitrile molecule. Chloride acts as a bridge between the two Fe(II) atoms. The crystallographically imposed C_4 axis contains the atoms N(2,3), Fe(4,5), and Cl(1). Evidently, the reduced nature of the cubanes renders the carbonyl-type oxygen atoms of Meida sufficiently basic to function as ligands. The overall cluster topology of **7** has not been previously encountered. Four cubane-type clusters in one molecule have been observed previously only in [$Fe_{16}S_{16}$(PR_3)$_8$][6] where the clusters are edge-fused rather than bridged in the manner of **7**.

Particularly interesting features of reduced clusters are the dimensions of the [$MoFe_3S_4$]$^{2+}$ cores. The situation is most simply summarized by the mean values of four bond lengths for oxidized and reduced clusters in Table 4; values in parentheses are standard deviations from the mean. Note that

Table 3. Interatomic Distances (Å) and Angles (deg) for the Tetrakis (μ_3:η^4-iminodicarboxylato) μ-Chloro Diacetonitrile Diiron Motif in [**7**]$(BPh_4)_3 \cdot 2CH_3CN$[a,b]

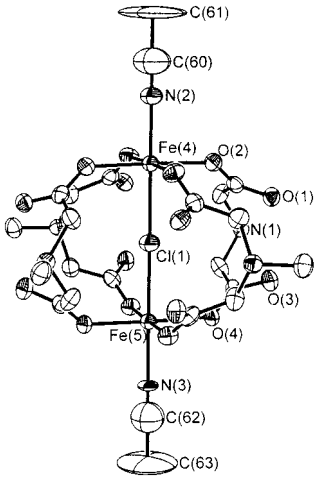

Fe(4)−O(2)	2.090(5)
Fe(4)−N(2)	2.11(1)
Fe(4)−Cl(1)	2.512(4)
O(2)−Fe(4)−N(2)	90.7(1)
O(2)−Fe(4)−Cl(1)	89.3(1)
O(2)−Fe(4)−Cl(2″)	89.99(1)
N(2)−Fe(4)−Cl(1)	180.00(1)
Fe(5)−O(4)	2.096(4)
Fe(5)−N(3)	2.09(1)
Fe(5)−Cl(1)	2.526(4)
N(3)−Fe(5)−O(4)	90.90(1)
O(4)−Fe(5)−Cl(1)	89.10(1)
O(4′)−Fe(5)−O(4‴)	89.99(1)
N(3)−Fe(5)−Cl(1)	180.00(1)

[a] Symmetry transformations used to generate equivalent atoms: (′) $y, -x + 1/2, z$; (″) $-x + 1/2, -y + 1/2, z$; (‴) $-y + 1/2, x, z$. [b] Structure is depicted with 50% probability ellipsoids.

$[(Cl_4cat)(MeCN)MoFe_3S_4(PBu^t_3)_3]$

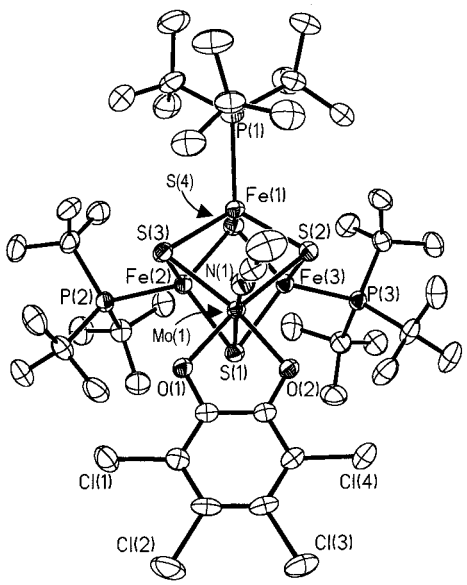

Figure 2. Structure of cluster **3** showing 50% probability ellipsoids and the atom-labeling scheme. The structure of **4** (excluding phosphine substituents) is essentially identical.

the ligand composition of **10** is closely related to that of **1**, the precursor of **3**−**5**; the cluster was selected for that reason. Tabulated values are averages of all distances of a given type,

$[(Cl_4cat)_2(Et_3P)_2Mo_2Fe_6S_8(PEt_3)_4]$

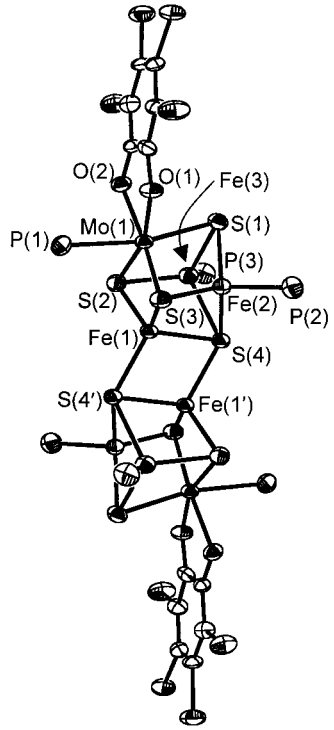

Figure 3. Structure of double cubane **5** showing 50% probability ellipsoids and the atom-labeling scheme. The cluster has a crystallographic inversion center.

$[\{(Meida)MoFe_3S_4(PCy_3)_3\}_4Fe_2(\mu\text{-}Cl)(MeCN)_2]^{3+}$

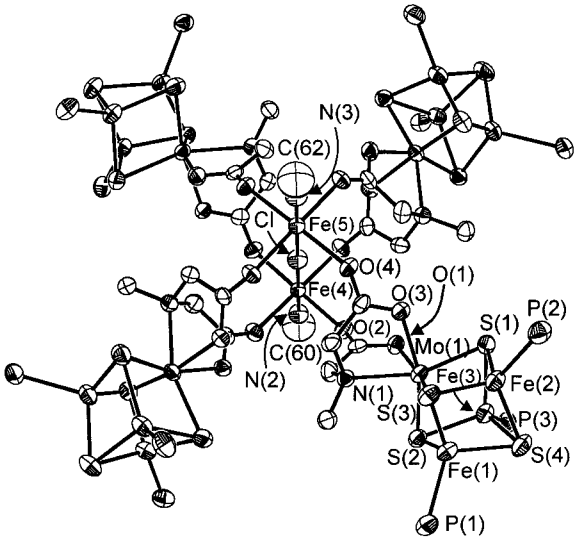

Figure 4. Structure of tetracubane **7** showing 50% probability ellipsoids and the atom-labeling scheme. The cluster has a crystallographic C_4 axis.

whether or not symmetry-related. Within the set of reduced clusters, Fe−Fe separations show a mild trend, decreasing in the order of decreasing phosphine cone angle: **3** > **7** ≳ **4** ≈ **5**. The origin of this trend may be steric. However, external P−Fe−S angles, a potential measure of structural distortions at iron sites, are too variable within and among clusters to discern any trend in phosphine-induced core distortion. Of somewhat more interest are differences between oxidized and reduced clusters. The Mo−S and Fe−S bond lengths are essentially invariant to oxidation state, but Mo−Fe and Fe−Fe separations

Table 4. Comparisons of Mean Values of Core Dimensions (Å) in Oxidized and Reduced Clusters

	Mo−Fe	Fe−Fe	Mo−S	Fe−S
		$[MoFe_3S_4]^{3+}$		
2[a]	2.730(6)	2.73(3)	2.35(1)	2.269(8)
10[b]	2.78(2)	2.728(5)	2.36(2)	2.28(1)
		$[MoFe_3S_4]^{2+}$		
3	2.71(1)	2.693(3)	2.360(3)	2.27(2)
4	2.68(1)	2.62(2)	2.36(3)	2.25(2)
5	2.67(1)	2.62(2)	2.39(3)	2.27(5)
7	2.67(1)	2.64(3)	2.36(1)	2.26(2)

[a] Reference 24. [b] Reference 22.

are not. These distances are invariably smaller in the reduced clusters, and in some cases (e.g., **10** vs **4**) the difference approaches 0.1 Å. This trend is opposite to that always observed for $[Fe_4S_4]^{2+,+}$ clusters.[26,27] A pertinent case is $[Fe_4S_4(SPh)_2(PBu^t_3)_2]$ (2.740(5) Å) vs $[Fe_4S_4(PBu^t_3)_3Cl]$ (2.768(9) Å),[5] where the indicated mean Fe−Fe distance is marginally longer in the $[Fe_4S_4]^+$ cluster. The bond contraction observed in reducing **1** to **3**/**4** implies that the added electron occupies an orbital with metal−metal bonding character. Such an assertion requires that chloride and phosphine do not have significantly different intrinsic effects on structure in the same core oxidation state, a difficult matter to prove.[28] We note, however, that the mixed-ligand species $[Fe_4S_4(SPh)_2(PBu^t_3)_2]$[5] exhibits dimensions entirely normal for $[Fe_4S_4]^{2+}$ clusters with non-phosphine ligation. In the present context, it is worth mentioning the apparent contractions of average metal−metal separations in the MoFe holoprotein of nitrogenase determined by EXAFS[29] and X-ray diffraction.[30] The effects are, however, near the error limits. A recent EXAFS study of a cofactor-deficient MoFe protein mutant reveals distance changes over two oxidation states that are not considered to be statistically significant.[31] When the precision of individual distances (Table 2) is taken into account under a 3σ criterion, the majority of differences in Table 4 are significant.

Oxidation States. (a) Electron Distribution. While chemical composition requires the $[MoFe_3S_4]^{2+}$ oxidation level for clusters **3**−**5**, the situation with tetracubanes **6** and **7** is not clear because of the presence of the two central iron atoms. Consequently, we have determined the zero-field Mössbauer spectra of clusters **3**−**7** to define oxidation states and discern the effects of tertiary phosphine ligands on spectral parameters. Mössbauer spectra of **4**−**7** are set out in Figure 5. Spectra were simulated as superpositions of quadrupole doublets with the isomer shifts (δ) and quadrupole splittings (ΔE_Q) in Table 5.

The spectrum of single cubane **4** at 4.2 K consists of two quadrupole doublets with very different ΔE_Q values; that of **3** (not shown) is very similar. The spectrum of double cubane **5** also consists of two quadrupole doublets but is less well-resolved owing to a smaller difference in quadrupole splittings. These spectra were best fit with quadrupole doublets very close to a

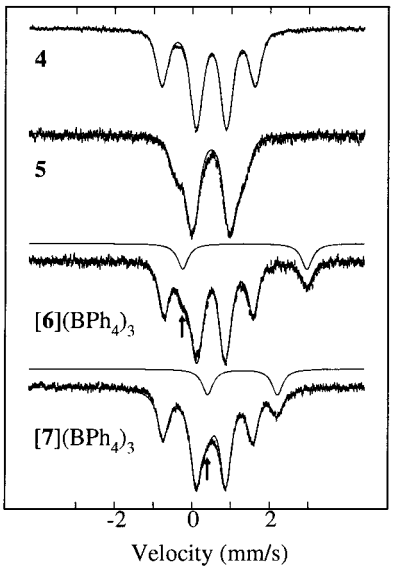

Figure 5. Zero-field spectra of the polycrystalline compounds **4**, **5**, [**6**](BPh$_4$)$_3$, and [**7**](BPh$_4$)$_3$. The solid lines drawn through the experimental data represent the sum of quadrupole doublets with the parameters given in Table 5. The solid lines above the data represent the contributions of the octahedral high-spin ferrous sites to the spectra of **6** and **7**.

2:1 intensity ratio, consistent with idealized C_s symmetry of the cubanes. Comparison of the spectra of **6** and **7** with the spectrum of **4** allows ready identification of the four lines for the quadrupole doublets of the $[MoFe_3S_4]^{2+}$ core. In addition, a new absorption line is present at the high-energy side of each spectrum. Closer inspection reveals the presence of the shoulders (marked by arrows) on the left (**6**) and right (**7**) of the low-energy absorption line of the most intense quadrupole doublet. Spectral analysis leads to the conclusion that the two new absorption lines in each spectrum belong to quadrupole doublets with $\delta = 1.35$ mm/s and $\Delta E_Q = 3.20$ mm/s for **6** and $\delta = 1.30$ mm/s and $\Delta E_Q = 1.80$ mm/s for **7**. These doublets, which are plotted above the experimental spectra, account for ∼15% of the iron in the clusters and, based on cluster composition established from the X-ray structure, can only represent the central pair of iron atoms in each cluster. Isomer shifts unambiguously identify these iron sites as high-spin Fe(II) with octahedral N/O coordination. Values of ΔE_Q typical of high-spin non-heme Fe(II) sites are usually larger than 2 mm/s.[32] However, $\Delta E_Q = 1.80$ mm/s for the octahedral Fe(II) sites of **7** is not an unprecedented low value in distorted cubic coordination. For example, the $Fe^{II}(SR)_6$ site of $[Mo_2Fe_7S_8(SEt)_{12}]^{4-}$ has $\Delta E_Q = 1.90$ mm/s,[33] and the (distorted tetrahedral) Fe(II) sites in the all-ferrous Fe_4S_4 cluster of the iron protein of nitrogenase have $\Delta E_Q = 1.24-1.70$ mm/s.[34] Once the oxidation state of the central $Fe_2(\mu\text{-Cl})$ unit is determined as 3+, the individual cluster oxidation state in **6** and **7** is unambiguously specified as $[MoFe_3S_4]^{2+}$.

Isomer shifts for the clusters reported herein span the relatively narrow interval 0.40−0.53 mm/s (Table 5). Conclusions about oxidation state based on isomer shifts have to be drawn with careful consideration of the influence of terminal ligands on this parameter. Phosphine coordination usually leads

(26) Berg, J. M.; Holm, R. H. In *Iron-Sulfur Proteins*; Spiro, T. G., Ed.; Wiley-Interscience: New York, 1982; Chapter 1.
(27) Carney, M. J.; Papefthymiou, G. C.; Frankel, R. B.; Holm, R. H. *Inorg. Chem.* **1989**, *28*, 1497.
(28) Cluster **1** has not been structurally characterized. For the closely related cluster **10**,[22] the mean Mo−Fe and Fe−Fe distances are 2.78(2) and 2.728(5) Å, respectively.
(29) Christiansen, J.; Tittsworth, R. C.; Hales, B. J.; Cramer, S. P. *J. Am. Chem. Soc.* **1995**, *117*, 10017.
(30) Peters, J. W.; Stowell, M. H. B.; Soltis, S. M.; Finnegan, M. G.; Johnson, M. K.; Rees, D. C. *Biochemistry* **1997**, *36*, 1181.
(31) Musgrave, K. B. Liu, H. I.; Ma, L.; Burgess, B. K.; Watt, G.; Hedman, B.; Hodgson, K. O. *J. Biol. Inorg. Chem.* **1998**, *3*, 344.
(32) Münck, E. In *Physical Methods in Inorganic and Bioinorganic Chemistry*; Que, L., Jr., Ed.; University Science Books: Sausalito, CA, 2000; Chapter 6.
(33) Wolff, T. E.; Power, P. P.; Frankel, R. B.; Holm, R. H. *J. Am. Chem. Soc.* **1980**, *102*, 4694.
(34) Angove, H. C.; Yoo, S. J.; Burgess, B. K.; Münck, E. *J. Am. Chem. Soc.* **1997**, *119*, 8730.

Table 5. Zero-Field 4.2 K Mössbauer Parameters of Clusters

cluster		mm/s δ^a	mm/s $\Delta E_Q{}^b$	% area
$[(Cl_4cat)(MeCN)MoFe_3S_4(PBu^t{}_3)_3]$	(**3**)	0.53	0.75	63
		0.51	2.27	37
$[(Cl_4cat)(MeCN)MoFe_3S_4(PPr^i{}_3)_3]$	(**4**)	0.49	0.78	65
		0.41	2.41	35
$[Mo_2Fe_6S_8(PEt_3)_6(Cl_4cat)_2]$	(**5**)	0.48	0.96	70
		0.45	1.72	30
$[\{MeidaMoFe_3S_4(PCy_3)_3\}_4Fe_2(\mu\text{-}Cl)(THF)_2](BPh_4)_3$	(**6**)	0.48	0.72	55
		0.42	2.30	29
		1.35	3.20	16
$[\{MeidaMoFe_3S_4(PCy_3)_3\}_4Fe_2(\mu\text{-}Cl)(MeCN)_2](BPh_4)_3$	(**7**)	0.49	0.76	58
		0.41	2.32	29
		1.30	1.80	15

[a] Typical precision ±0.02 mm/s. [b] Typical precision ±0.03 mm/s.

to isomer shifts smaller than those for thiolate-coordinated iron sites in the same oxidation state. Therefore, $[Fe_4S_4(PR_3)_4]^+$ clusters (R = Pr^i, Cy, Bu^t), which contain the $[Fe_4S_4]^+$ core, and $[Fe_8S_8(PCy_3)_6]$, with two bridged $[Fe_4S_4]^0$ cores,[6] represent good comparison systems for the present clusters. The average isomer shifts for **4** (0.46 mm/s), **6** (0.46 mm/s), and **3** (0.51 mm/s) are very similar to those of $[Fe_4S_4(PR_3)_4]^+$ (at 77 K) with the same phosphine: R = Pr^i, 0.46 mm/s; R = Cy, 0.48 mm/s; R = Bu^t, 0.51 mm/s. These values are smaller than that for the all-ferrous cluster $[Fe_8S_8(PCy_3)_6]$ (0.57 mm/s). These results, together with the average oxidation of 2.25+ in $[Fe_4S_4]^+$ clusters, suggest that the $[MoFe_3S_4]^{2+}$ clusters analyzed herein can be formulated as $[Mo^{3+}Fe^{2+}{}_2Fe^{3+}]$.

Recent ^{57}Fe Q-band ENDOR studies of the iron−molybdenum cofactor of nitrogenase in the resting ($S = 3/2$) state leads to the proposal of the highly reduced $[Mo^{4+}Fe^{2+}{}_6Fe^{3+}]$ oxidation level.[35] In this state the iron sites have $\delta_{av} = 0.41$ mm/s and $\Delta E_{Qav} = 0.76$ mm/s.[36] Isomer shifts in the resting, one-electron reduced, and one-electron oxidized states occur in the interval 0.35 to 0.49 mm/s. While there are differences in coordination number and terminal ligands between the cofactor and the reduced clusters examined here, we note the similarity in isomer shifts. These results may offer some support for a strongly reduced cofactor, possibly approaching the all-ferrous condition.

(b) Accessible States. Prior to examining the electrochemical properties of the clusters, attention is directed to the ^{1}H NMR spectra in Figure 6. The $[MoFe_3S_4]^{2+}$ clusters **3**−**7** are expected to have an $S = 2$ ground state established for **8**.[37] Consequently, all clusters exhibit isotropically shifted spectra. Despite idealized C_s symmetry, **3** and **4** in chloroform show equivalent phosphine ligands and thus are fluxional. The dynamic process may involve phosphine exchange between inequivalent sites and/or dissociation and rebinding of the acetonitrile ligand, with attendant reorientation of the catecholate ring so as to give averaged trigonal symmetry. The latter process has been observed previously.[22] When a solution of **3** is cooled, the Bu^t signal originally at δ 6.70 shifts and broadens. At ca. 250 K, two signals are observed at δ 5.1 and 12.2, corresponding to the two inequivalent iron sites. The spectrum of **5** in chloroform shows well-separated Mo−PEt$_3$ and Fe−PEt$_3$ resonances. Methylene protons at the four equivalent iron sites are diastereotopic and occur as two equally intense resonances separated by 2.4 ppm. Diastereotopic methylene splitting of thiolate ligands at iron sites is occasionally resolved in paramagnetic MFe_3S_4 clusters.[38,39] The spectrum of **7** in dichloromethane consists of diastereotopic methylene group signals of the Meida ligand at low field, a set of cyclohexyl signals of the PCy$_3$ ligands, and a probable N−Me resonance at δ −1.0. Because of its closer proximity to the cluster, the methine protons are assigned to the most downfield cyclohexyl signal (δ 5.78). The spectra are at least consistent with the solid state structures.

Accessible oxidation states of **3**−**7** have been examined by cyclic voltammetry. The voltammogram of double cubane **5** in Figure 7 reveals a chemically reversible oxidation at −0.06 V and reduction at −0.77 V in dichloromethane ($i_{pc}/i_{pa} \approx 1$). An earlier report described these processes as irreversible.[16] Voltammograms of **6** and **7** in dichloromethane (not shown) are identical and reveal irreversible oxidations (0.24, 0.80 V) and an irreversible reduction (−1.5 V). The redox behavior of **3** and **4** is particularly well-developed. The voltammograms of both single cubanes, presented in Figure 7, reveal three chemically reversible steps corresponding to the four-member electron transfer series 4 with steps E_1, E_2, and E_3 specified in Figure 8. When compared with anionic thiolate-ligated clusters **9**, **11**, and others,[40,41] stabilization of the $[MoFe_3S_4]^{2+,+}$ states is evident. The $[MoFe_3S_4]^+$ state can be reached at $E_1 \approx -1.2$ V; this state has not been observed with any anionic cluster thus far. The highly oxidized $[MoFe_3S_4]^{4+}$ state has been observed with all four clusters; the highly positive potential $E_3 \approx 1.0$ V is required with **3** and **4**. Overall, the effect of PR$_3$ substitution of anionic ligands is to shift potentials in the positive direction. This behavior follows from the removal of cluster negative charge and the usual tendency of phosphines to support lower oxidation states. Values of E_1 and E_2 suggest that, in addition to the $[MoFe_3S_4]^{2+}$ state, the $[MoFe_3S_4]^{+,3+}$ levels of phosphine-ligated clusters should be isolable.

Tertiary Phosphines as Reductants. As observed at the outset, the probable reductant in the syntheses of $[Fe_4S_4(PR_3)_3L]^{+,0}$ and **5** is the phosphine. While not generally used as reductants, tertiary phosphines and phosphites have found application in the synthesis of low-valent complexes. A number of these are homoleptic M(0) complexes of the group 10 metals, prepared from metal salts in nonalcoholic solvents. The initial results with phosphines are those of Malatesta,[42] who demonstrated the formation of Ph_3PO in a $Pd(NO_3)_2$ reaction system

(35) Lee, H.-I.; Hales, B. J.; Hoffman, B. H. *J. Am. Chem. Soc.* **1997**, *119*, 11395.
(36) Huynh, B. H.; Henzl, M. T.; Christner, J. A.; Zimmermann, R.; Orme-Johnson, W. R.; Münck, E. *Biochim. Biophys. Acta* **1980**, *623*, 124.
(37) Mascharak, P. K.; Papaefthymiou, G. C.; Armstrong, W. H.; Foner, S.; Frankel, R. B.; Holm, R. H. *Inorg. Chem.* **1983**, *22*, 2851.
(38) Ciurli, S.; Carrié, M.; Holm, R. H. *Inorg. Chem.* **1990**, *29*, 3493.
(39) Ciurli, S.; Holm, R. H. *Inorg. Chem.* **1991**, *30*, 743.
(40) Mascharak, P. K.; Armstrong, W. H.; Mizobe, Y.; Holm, R. H. *J. Am. Chem. Soc.* **1983**, *105*, 475.
(41) Armstrong, W. H.; Mascharak, P. K.; Holm, R. H. *J. Am. Chem. Soc.* **1982**, *104*, 4373.
(42) Malatesta, L.; Angoletta, M. *J. Chem. Soc.* **1957**, 1186.

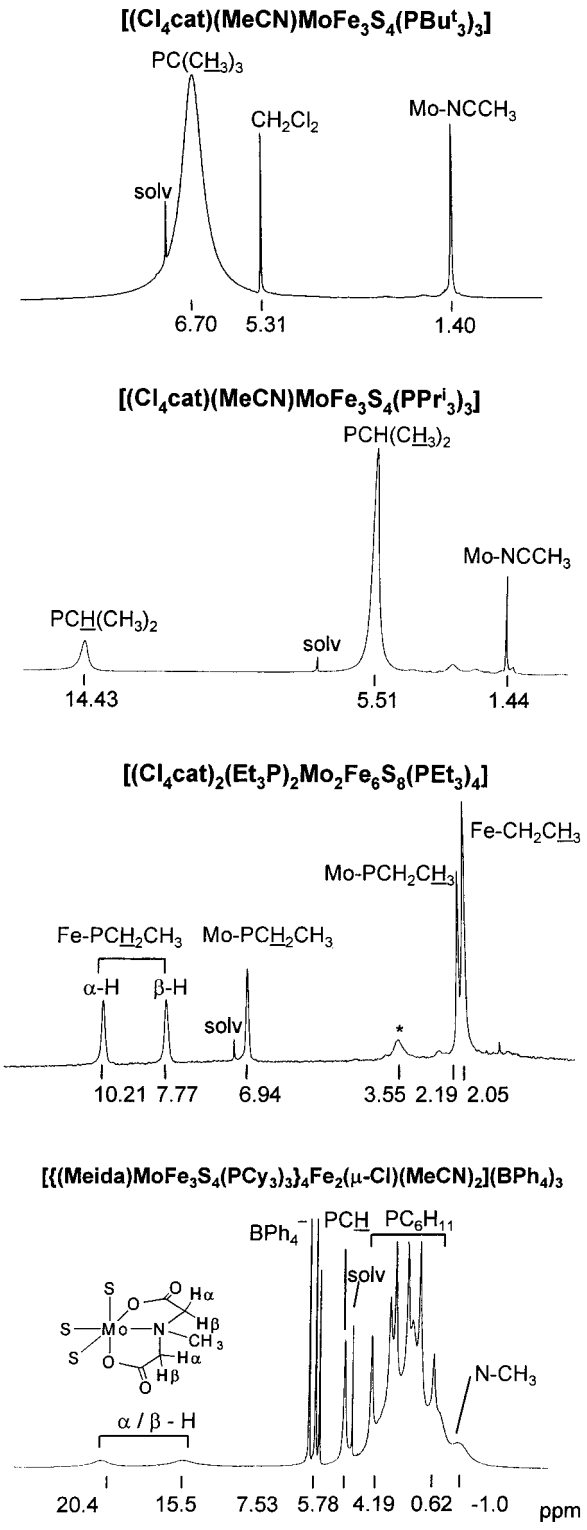

Figure 6. ^{1}H NMR spectra of clusters **3**, **4**, and **5** in $CDCl_3$ and of cluster **7** in CD_2Cl_2; signal assignments are indicated.

in benzene which afforded $[Pd(PPh_3)_4]$. Very recently, the formation of phosphine oxide has been demonstrated by ^{31}P NMR when Pd(0) complexes are prepared in toluene from $Pd(OAc)_2$.[43] The compounds $[M(pta)_4]$ with M = Ni, Pd, Pt have been synthesized from $M^{II}Cl_2$ salts in water using an excess of the water-soluble phosphine pta.[44] The phosphite complexes $[M(P(OEt)_3)_4]$ have been obtained in an analogous manner.[45,46]

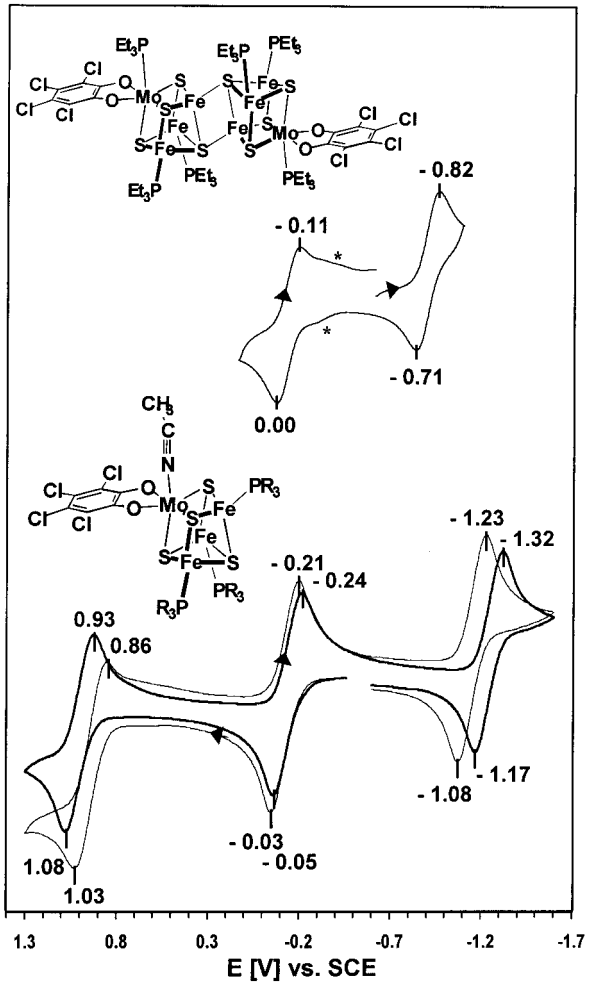

Figure 7. Cyclic voltammograms in dichloromethane demonstrating the four-member electron transfer series of monocubanes **3** and **4** (100 mV/s, lower) and the three-member series of double cubane **5** (300 mV/s, upper); peak potentials vs SCE are indicated. Features identified with asterisks (*) arise from the reduction process at −0.77 V.

Where water is the source of oxygen, the reductive half-reaction for phosphines is $R_3P + H_2O \rightleftharpoons R_3PO + 2H^+ + 2e^-$. We are unaware of a reported potential for this reaction.

To examine R_3P as a possible reductant in the formation of reduced Fe_4S_4 clusters, a system with the idealized stoichiometry of reaction 3 was investigated. Here it is assumed that 1 equiv of phosphine will react with one cluster to form phosphine sulfide and two electrons, one of which is utilized in forming the product cluster and the other of which is taken up by the fictitious cluster. Accordingly, 2 equiv (0.043 mmol) of the initial cluster salt was reacted with 5 equiv of the phosphine in 2 mL of acetonitrile. After 30 min, the ^{31}P NMR spectrum showed two signals with the integrated ratio δ 30 (Ph_4P^+):δ 79 (Pr^i_3PS) = 4.0. An authentic sample of Pr^i_3PS was prepared by modification of a reported procedure[47,48] to confirm the NMR assignment. The compound was purified by sublimation and identified by an X-ray structure determination.[49] The observed

(43) Csákai, Z.; Skoda-Földes, R.; Kollár, L. *Inorg. Chim. Acta* **1999**, *286*, 93.
(44) Darensbourg, D. J.; Robertson, J. B.; Larkins, D. L.; Reibenspies, J. H. *Inorg. Chem.* **1999**, *38*, 2473.
(45) Vinal, R. S.; Reynolds, L. T. *Inorg. Chem.* **1964**, *3*, 1062.
(46) Meier, M.; Basolo, F.; Pearson, R. G. *Inorg. Chem.* **1969**, *8*, 795.
(47) Cowley, A. H.; Mills, J. L. *J. Am. Chem. Soc.* **1969**, *91*, 2915.
(48) Shaw, C. F., III; Isab, A. A.; Hoeschele, J. D.; Starich, M.; Locke, J.; Schulties, P.; Xiao, J. *J. Am. Chem. Soc.* **1994**, *116*, 2254.
(49) Pr^i_3PS (213 K) : monoclinic, *C*/*c*, a = 18.498(4) Å, b = 12.640(2) Å, c = 12.639(2) Å, β = 132.98(1) °, Z = 8, V = 2373(1) Å^3.

REDOX SERIES OF $[MoFe_3S_4]$ CLUSTERS[a]

	$[MoFe_3S_4]^{4+}$	E_3	$[MoFe_3S_4]^{3+}$	E_2	$[MoFe_3S_4]^{2+}$	E_1	$[MoFe_3S_4]^{1+}$ (4)
3[b]		1.01		-0.15		-1.25	
4[b]		0.95		-0.12		-1.16	
11[c]		-0.08		-1.02		---	
9[c]		~0.4[d]		-1.07		---	

[a] V vs. SCE, 298 K. [b] CH_2Cl_2. [c] MeCN, ref 40. [d] Irreversible.

Figure 8. The four-member electron transfer series of $MoFe_3S_4$ clusters, with potentials for the indicated clusters. Examples of $[MoFe_3S_4]^{+,4+}$ clusters have not yet been isolated.

NMR intensity ratio conforms to reaction 3. In practice, the preparation of $[Fe_4S_4(PR_3)_4]^+$ clusters was conducted with excess phosphine using the mole ratio $[Fe_4S_4Cl_4]^{2-}$:R_3P:$NaBPh_4$ = 4.4:1.0:4.0.[6]

$$2(Ph_4P)_2[Fe_4S_4Cl_4] + 5Pr^i_3P \rightarrow [Fe_4S_4(PPr^i_3)_4]^+ + Pr^i_3PS + 4Ph_4PCl + \text{“}[Fe_4S_3Cl_4]^-\text{”} \quad (3)$$

In a second experiment modeled after reaction 1, a system with the mole ratio **1**:Pr^i_3P:$NaBPh_4$ = 1.0:3.5:3.0 on a 0.048 mmol scale of initial cluster in 2 mL of acetonitrile was allowed to react for 30 min. The solvent was removed, and the black residue was extracted with benzene. Using calibrated coaxial tubes and Ph_3PO (δ 25.5, benzene) as an external standard, the quantity of Pr^i_3PS formed was determined by integration of ^{31}P NMR spectra. The reaction system was devised assuming that 3 equiv of phosphine substitutes for the three chloride ligands of **1** and $^1/_2$ equiv of phosphine generates the electron required for the formation of cluster **4**. On this basis, an average of 59% of phosphine sulfide was recovered in three separate experiments. We are uncertain as to the cause of the low values. However, this experiment and that based on reaction 3 demonstrate that most or, more likely, all of the reducing equivalents result from phosphine oxidation. The formal half-reaction is $R_3P + S^{2-} \rightleftarrows R_3PS + 2e^-$. We are unaware of any reported potential for this reaction or for that involving HS^-.

Summary

The following are the principal results and conclusions of this investigation.

1. The reaction systems $[(Cl_4cat)(MeCN)MoFe_3S_4Cl_3]^{2-}$ (**1**)/4.0−4.5PR_3/3$NaBPh_4$ in acetonitrile afford the clusters $[(Cl_4cat)(MeCN)MoFe_3S_4(PR_3)_3]$ (R = Bu^t (**3**), Pr^i (**4**)) and $[(Cl_4cat)_2(Et_3P)_2Mo_2Fe_6S_8(PEt_3)_4]$ (**5**, previously reported[16]). The related system $[(Meida)MoFe_3S_4Cl_3]^{2-}$ (**2**)/5PCy_3/4$NaBPh_4$ forms the tetracubanes $[\{(Meida)MoFe_3S_4(PCy_3)_3\}_4Fe_2(\mu\text{-}Cl)L_2]^{3+}$ (L = THF (**6**), MeCN (**7**)). In these systems, the $[MoFe_3S_4]^{3+}$ cores of precursor clusters **1** and **2** are reduced to the $[MoFe_3S_4]^{2+}$ level.

2. X-ray crystallographic analysis reveals single-cubane structures for **3** and **4**, whose principal structural feature is metal−metal separations shorter than in **1** and other oxidized ($[MoFe_3S_4]^{3+}$) clusters. The reverse trend is always observed in $[Fe_4S_4]^{2+,+}$ clusters. Cluster **5** possesses a rhomboidal-bridged centrosymmetric double-cubane structure (reported earlier in a different space group[16]), very similar to that of $[Fe_8S_8(PR_3)_6]$. Clusters **6** and **7** are tetracubanes in which four Meida oxygen atoms from different cubanes bind each of two central high-spin Fe(II) atoms in *trans*-Fe(μ-Cl)LO_4 coordination. The overall topology of these clusters is not precedented.

3. Average isomer shifts of **3**−**7** (0.46−0.52 mm/s) are larger than those of typical thiolate-ligated oxidized clusters such as $[(al_2cat)(RS)MoFe_3S_4(SR)_3]^{3-}$ (**9**) (0.42 mm/s). Although data are limited, phosphine vs thiolate ligation at the same cluster oxidation level reduces isomer shifts. The formulation $[Mo^{3+}Fe^{2+}{}_2Fe^{3+}S_4]$ for reduced clusters is suggested by isomer shift data.

4. Clusters **3** and **4** exhibit the four-member electron transfer series traversing the core oxidation states $[MoFe_3S_4]^{4+,3+,2+,+}$ over the potential interval of ca. −1.2 to +1.0 V vs SCE. Compared to the clusters with monoanionic ligands at the iron sites (e.g., **9**), phosphine ligation shifts the potential scale to more positive values; i.e., reduced clusters are increasingly stabilized. This effect arises from removal of cluster negative charge and the tendency of phosphines to stabilize lower oxidation states.

5. The reducing agent in the synthesis of reduced phosphine-ligated clusters from oxidized clusters, viz., $[Fe_4S_4(PR_3)_4]^+$ from $[Fe_4S_4Cl_4]^{2-}$ ($[Fe_4S_4]^{2+} + e^- \rightarrow [Fe_4S_4]^+$), and **3**, **4**, **5** from **1** and **6**, **7** from **2** ($[MFe_3S_4]^{3+} + e^- \rightarrow [MFe_3S_4]^{2+}$) is the tertiary phosphine. Electrons are generated in the formal half-reaction $R_3P + S^{2-} \rightleftarrows R_3PS + 2e^-$ of unknown potential.

Acknowledgment. This research was supported by NIH Grant GM 28856. F.O. is grateful to the Deutsche Forschungsgemeinschaft (DFG) for a postdoctoral fellowship. We thank Dr. R. Koerner for discussions and experimental assistance and Dr. R. J. Staples for consultation on crystallography.

Supporting Information Available: Four X-ray crystallographic files in CIF format for the compounds in Table 1. This material is available free of charge via the Internet at http://pubs.acs.org.

IC991016X